Optimal broadband antireflective taper

Yinan Zhang,[1,*] Changlin Li,[2] and Marko Loncar[1]

[1]*School of Engineering and Applied Sciences, Harvard University, Cambridge, Massachusetts 02138, USA*

[2]*Harvard College, Harvard University, University Hall, Cambridge, Massachusetts 02138, USA*

**Corresponding author: yinan@seas.harvard.edu*

Received December 6, 2012; revised January 20, 2013; accepted January 25, 2013;
posted January 25, 2013 (Doc. ID 181267); published February 22, 2013

We have solved the optimal taper design for minimizing reflection over a broad frequency band for a given tapered length. We believe this work will lead to significant improvement in developing broadband antireflective devices in many areas.

OCIS codes: 310.1210, 310.6805, 050.6624.

Reflection of a wave traveling from one medium into another is a familiar concept in disciplines as diverse as electromagnetism, acoustics, and seismology. Minimizing the reflectance, caused by impedance mismatch, is therefore an extremely important issue in many fields. Impedance matching can be realized with the aid of interference. The quarter-wave coating on optical lenses and the quarter-wave impedance transformer used in electrical transmission lines offer classic examples. However, interference-based devices, by their nature, only operate within a narrow bandwidth, and in the case of optics over limited range of incident angles.

Alternatively, a broadband impedance matching can be achieved by adiabatically coupling the wave from one medium to another through a graded-impedance taper. For example, in acoustics, horns are used to increase the sound coupling of the human voice or musical instruments to open space. In optics, the tapered interface layer, with continuously varying impedance, can be realized by structuring the interface between two media, at a scale considerably smaller than the wavelength (λ) of interest. An example of such a structured interface can be found in natural biological systems, including dragonfly wings [1] and moth eyes [2,3].

The performance of the taper is dependent on its tapered length (l), as well as the tapered impedance profile [4,5]. As the tapered length increases with respect to λ, reflection can be reduced because of smoother adiabatic conversion. However, in practical realization, the tapered length is often limited by fabrication and/or other implementation constraints.

In this Letter, we seek the optimal impedance profile, which minimizes the reflectance across a broad frequency band for a given tapered length. Our approach is general and the results are applicable to a wide class of physical phenomena that involve wave propagation. For example, this work could lead to a significant performance improvement in stealth technology and photovoltaics [6,7].

The behavior of an electromagnetic wave propagating inside a medium with varied index can be described by 1D Maxwell's equations (in the time-harmonic form),

$$\begin{cases} \dfrac{d}{dx}E(x) = i\omega\mu(x)H(x) \\ \dfrac{d}{dx}H(x) = i\omega\epsilon(x)E(x) \end{cases}, \tag{1}$$

where μ and ϵ are the medium permeability and permittivity. The telegrapher's equations of transmission lines and acoustic equations follow the same form.

For further insight into Eq. (1), we perform the following normalization: we define the optical length of the tapered section to be $L = \int_0^l n(x)\mathrm{d}x$, where $n(x)$ is the material's refractive index. Next, we normalize the x axis with respect to its optical length. The normalized unit $u \in [0,1]$ is defined by $u = \int_0^x n(x')\mathrm{d}x'/L$. With this normalized unit u, Eq. (1) can be rewritten as

$$\begin{cases} \dfrac{dE}{du} = i2\pi\dfrac{L}{\lambda}\mathcal{Z}(u)H(u) \\ \dfrac{dH}{du} = i2\pi\dfrac{L}{\lambda}\dfrac{1}{\mathcal{Z}(u)}E(u) \end{cases}, \tag{2}$$

where $\mathcal{Z} = \sqrt{\mu/\epsilon}$ is the material impedance. From Eq. (2), the electromagnetic wave can be separated into a forward-propagating wave and a backward-propagating wave with a coefficient r,

$$r(u) = \frac{\mathcal{E}(u) - \mathcal{Z}(u)\mathcal{H}(u)}{\mathcal{E}(u) + \mathcal{Z}(u)\mathcal{H}(u)}. \tag{3}$$

Importantly, $r(0)$ describes the percentage of light in amplitude that reflects off from the $u = 0$ interface, and $r(1) = 0$ because we assume there is no backward-propagating light incident from the $u = 1$ interface.

Combining Eqs. (2) and (3) leads to a nonlinear ordinary differential equation (ODE) of $r(u)$:

$$\frac{dr}{du} + i4\pi\frac{L}{\lambda}r = -\frac{1}{2}(1 - r^2)p(u), \tag{4}$$

where $p = d\ \ln\ \mathcal{Z}/du$ contains the information of the tapered profile.

The goal is to find the optimal tapered function $p(u)$ that results in minimal $R = |r(0)|^2$ across a certain bandwidth $[\lambda_{\min}, \lambda_{\max}]$. First, we employ an approximation to solve this problem semi-analytically, and then we use numerical approaches to find the exact solutions. For a small r, using an approximation $r^2 \ll 1$, Eq. (4) can be reduced to a linear ODE, which has the exact solution

$$r(0) = \frac{1}{2}\int_0^1 p(u)\exp\left(i4\pi\frac{L}{\lambda}u\right)\mathrm{d}u. \tag{5}$$

Note that Eq. (5) is equivalent to Fourier transform (FT),

$$r(0) = P(2L/\lambda)/2, \tag{6}$$

where $P(2L/\lambda)$ is the FT of $p(u)$, and $2L/\lambda$ corresponds to the frequency of the FT. It is important to note that $P(0)$ is constrained by a constant for any tapered function $p(u)$, $P(0) = \int_0^1 p(u')\mathrm{d}u' = \ln \mathcal{Z}_2 - \ln \mathcal{Z}_1$, where $\mathcal{Z}_1$ and $\mathcal{Z}_2$ are the impedance of the two media. This is because $P(0)$ approximates the reflection between the two media without taper. Therefore the problem of finding the optimal tapered profile that has minimum reflectance at bandwidth $[\lambda_{\min}, \lambda_{\max}]$ given the optical length L is equivalent to finding the optimal window function $p(u)$, confined within $[0, 1]$, whose FT's sideband level R^* above cutoff frequency $f_c = L/\lambda_{\max}$ is minimal. $R^*(f_c)$ is defined as

$$R^*(f_c) = \max\left\{\left|\frac{P(f)}{P(0)}\right|_{f>f_c}\right\}. \tag{7}$$

Interestingly, the above-mentioned problem is analogous to the side-lobe suppression problem in signal processing [8]. Among the many window functions utilized in signal processing, the Dolph–Chebyshev window function satisfies the above-mentioned requirements for $p(u)$: it minimizes the sideband level $R^*(f_c)$ for given cutoff frequency f_c [9]. Historically, the Dolph–Chebyshev window has been used to optimize the directionality of the phase antenna [9], and to design a tapered section in an electrical transmission line [10]. In the latter case, the refractive index has been treated as constant throughout the taper, which is only valid for the TEM mode in a coaxial metal waveguide. In this Letter, we provide a generalized model for designing a broadband antireflective device.

In Fig. 1 we compare different tapered profiles, their respective window functions $p(u)$, and their reflectance spectra (in decibels) predicted by Eq. (5). As a concrete example, we choose to minimize the reflection between

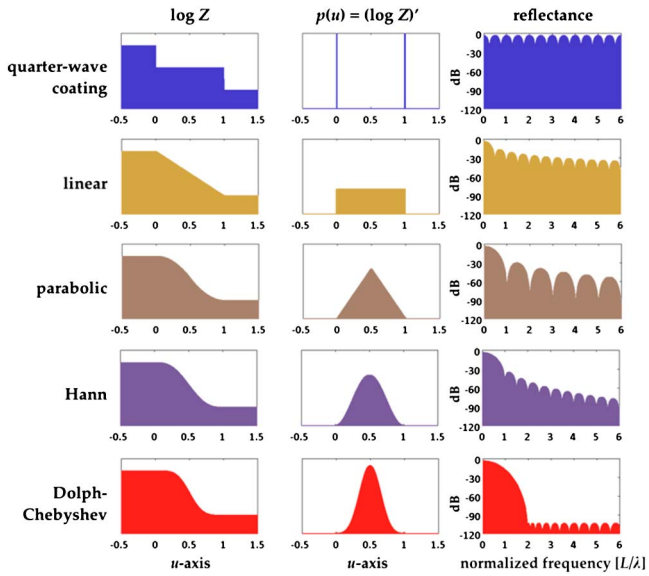

Fig. 1. (Color online) Comparison of different tapered profiles for antireflective coatings at silicon/air interface, and their respective reflectance predicted by the Fourier model.

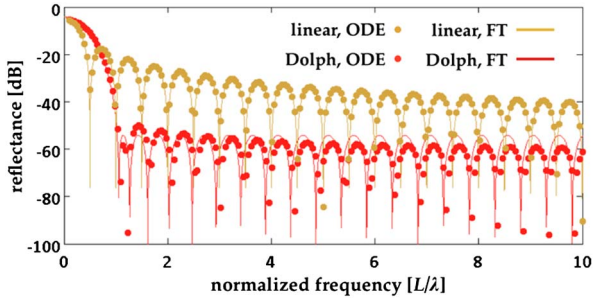

Fig. 2. (Color online) Comparison of power reflectance between that predicted by the Fourier model and that calculated by solving Maxwell's equations.

air ($n = 1$) and silicon ($n = 3.5$) at telecommunication wavelength. In the case of a quarter-wave coating, the step function in the impedance profile results in two Dirac delta functions in $p(u)$. Its FT is the result of beating between two constant-amplitude functions with a frequency difference, leading to zero reflectance at $L/\lambda = 1/4 + m/2$ for $m \in \mathbb{N}$, as expected for quarter-wave coating. At all other frequencies where this condition is not satisfied, the reflectance level remains high (30%, −5 dB).

On the other hand, when tapering is applied, reflectance side lobes can be suppressed over a wide normalized frequency range. For all tapered profiles except the Dolph–Chebyshev one, the height of the side lobes decreases as the normalized frequency increases. This is expected since for given wavelength of incident wave, larger normalized frequencies mean longer structure with gentler, more adiabatic, taper. The Dolph–Chebyshev taper, specially, can have significantly smaller and frequency-independent side lobes R_{sb} [9,11]. As an example, in Fig. 1 we plot a Dolph–Chebyshev function that is optimized for a cutoff frequency of $L/\lambda_{\max} = 2$ and has a sideband reflectance of $R_{sb} = -105$ dB.

Having identified the Dolph–Chebyshev tapered profile as the most promising one, in Fig. 2 we evaluate the validity of our modeling. We compare the analytical solution predicted by the Fourier model [with the r^2 approximation in Eq. (4)] with the numerical solution to Eq. (4). In Fig. 2, the result derived from the FT is plotted with a solid curve, while that produced by the numeric solution is plotted with dots. Here, different from the

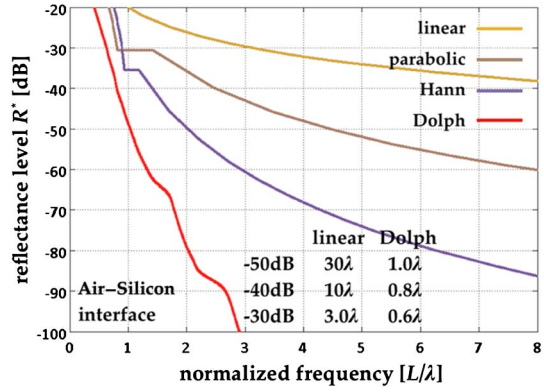

Fig. 3. (Color online) Comparison of different tapered functions' performances, for air/silicon interface as an example.

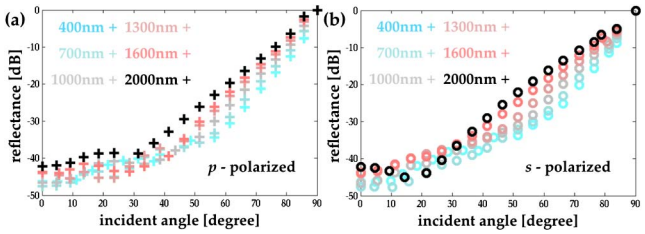

Fig. 4. (Color online) (a),(b) Reflectance dependence on incident angle, at different wavelengths across the solar spectrum, for p- and s-polarized light.

one in Fig. 1, the Dolph–Chebyshev function is optimized for a cutoff frequency of $L/\lambda_{\max} = 1$ and has a sideband reflectance of $R_{\text{sb}} = -55$ dB. Figure 2 shows that the Fourier model prediction is in good agreement with the simulation.

Next, in Fig. 3, we compare the reflectance level $R^*(f_c)$ of Dolph–Chebyshev taper to other taper functions, calculated with the numerical solution. It can be seen that the Dolph–Chebyshev taper outperforms the other impedance profiles. The difference in performance becomes increasingly dramatic as the desired R^* decreases. For example, in order to reach a reflectance level of –50 dB, implementing with a linear taper requires an optical length L longer than 30λ; the same reflectance can be achieved with a Dolph–Chebyshev taper of an optical length L of only 1.0λ.

Finally, we provide an example of a broadband wide-angle antireflective coating with Dolph–Chebyshev taper using our theory. We aim to minimize the reflection loss between air and silicon [12] across the solar spectrum from 400 to 2000 nm, with $R^* = -48$ dB at normal incidence. To meet this condition, from Fig. 3, the optical length of the taper needs to satisfy $L \geq 1.0\lambda$. We choose $L = 1.25\lambda_{\max} = 2.50$ μm, which corresponds to a coating thickness of $l = 1.49$ μm. We performed two-dimensional finite-difference time-domain simulation in order to obtain reflectance at oblique incidence angle. In the simulation, the structure's refractive index only varies in the x direction. Figure 4 plots the reflectance spectra as a function of the incident angle at different wavelengths, for p- and s-polarized light, respectively. As shown in Fig. 4, our design not only demonstrates high antireflective property across the entire solar spectrum, as expected, but also performs well within a large incident angle range. The power loss from reflectance remains below 1% within an incident angle of 55° for both polarizations.

Various nanofabrication techniques have been demonstrated to fabricate such a textured interface, including focused ion beams [13], nanoimprint from bio-templates [14], dry etching with a self-assembled mask [15], colloidal lithography [7], and interference lithography [16]. The designed tapered profile can be realized with fine tuning of the etching parameters and/or leveraging etch-mask erosion.

In summary, we have demonstrated that Dolph–Chebyshev taper can achieve the same antireflective performance with much shorter cones, compared with other tapered functions. We believe this work will shed light on designs of broadband antireflective components in various areas.

The authors acknowledge support from the AFOSR Award No. FA9550-09-1-0669-DOD35CAP. Y. Zhang acknowledges the assistance provided by Shota Kita. Y. Zhang dedicates this work to the friendship with "the family."

References

1. I. R. Hooper, P. Vukusic, and R. J. Wootton, Opt. Express **14**, 4891 (2006).
2. P. B. Clapham and M. C. Hutley, Nature **244**, 281 (1973).
3. S. J. Wilson and M. C. Hutley, Opt. Acta **29**, 993 (1982).
4. B. Sheldon, J. S. Haggerty, and A. G. Emslie, J. Opt. Soc. Am. **72**, 1049 (1982).
5. E. B. Grann, M. G. Moharam, and D. A. Pommet, J. Opt. Soc. Am. A **12**, 333 (1995).
6. K. X. Wang, Z. Yu, V. Liu, Y. Cui, and S. Fan, Nano Lett. **12**, 1616 (2012).
7. H. L. Chen, S. Y. Chuang, C. H. Lin, and Y. H. Lin, Opt. Express **15**, 14793 (2007).
8. P. S. R. Diniz, E. A. B. da Silva, and S. L. Netto, *Digital Signal Processing: System Analysis and Design* (Cambridge University, 2002).
9. C. L. Dolph, Proc. IRE **34**, 335 (1946).
10. R. W. Klopfenstein, Proc. IRE **44**, 31 (1956).
11. P. Baumeister, Appl. Opt. **25**, 4568 (1986).
12. E. D. Palik, *Handbook of Optical Constants of Solids* (Academic, 1985).
13. T. Søndergaard, S. M. Novikov, T. Holmgaard, R. L. Eriksen, J. Beermann, Z. Han, K. Pedersen, and S. I. Bozhevolnyi, Nat. Commun. **3**, 969 (2012).
14. G. Xie, G. Zhang, F. Lin, J. Zhang, Z. Liu, and S. Mu, Nanotechnology **19**, 095605 (2008).
15. Y. Huang, S. Chattopadhyay, Y. Jen, C. Peng, T. Liu, Y. Hsu, C. Pan, H. Lo, C. Hsu, Y. Chang, C. Lee, K. Chen, and L. Chen, Nat. Nanotechnol. **2**, 770 (2007).
16. K. C. Park, H. J. Choi, C. H. Chang, R. E. Cohen, G. H. McKinley, and G. Barbastathis, ACS Nano **6**, 3789 (2012).